Global buckling strength of discretely fastened back-to-back built-up cold-formed steel columns

Akshay Mangal Mahar[1], S. Arul Jayachandran[2], Mahen Mahendran[3*]

[1]Joint Ph.D. Research scholar, Indian Institute of Technology Madras, India and Queensland University of Technology, Australia. E-mail: akshaymangalmahar@hdr.qut.edu.au (ORCID: 0000-0003-1088-9619)

[2] Professor, Department of Civil Engineering, Indian Institute of Technology Madras, Chennai 600036, India. E-mail: aruls@iitm.ac.in (ORCID: 0000-0002-1573-3050)

[3]Professor, School of Civil and Environmental Engineering, Queensland University of Technology, Brisbane 4000, Australia. E-mail: m.mahendran@qut.edu.au (*Corresponding author) (ORCID: 0000-0001-7306-8821)

Abstract

This study proposes a design equation for built-up CFS columns to eliminate the inconsistencies present in Section I1.2 of AISI-S100 specification. The proposed equation was developed by using the results from the authors' compound spline finite strip-based numerical framework and 228 experimental and numerical results from literature on built-up CFS columns, failing by minor axis buckling. Investigations were conducted using numerical models with mode-specific deformations incorporated in compound spline finite strip framework. The shear slip behaviour between the individual columns, characterised by (i) fastener spacing and (ii) slenderness ratio of fully-composite cross-section, was investigated using parametric variations. The study shows that the modified slenderness ratio (MSR) in Section I1.2 of AISI-S100 yields conservative strength predictions with increased fastener spacing. This is possibly because the MSR considers the effect of fastener spacing and overall slenderness ratio as disjoint and treat them as additive components. In reality, they interact, and hence a compound slenderness ratio (CSR) is proposed with a term that captures the interaction of these two entities. The prediction of strength by the proposed CSR and direct strength method (DSM) is in good agreement with the results of experimental and numerical studies, with the mean close to one. When incorporated in the DSM design equations, the proposed CSR yields matching reliability with AISI S100.

Keywords: Compound spline finite strip method; Cold-formed steel; Built-up section; Modified slenderness ratio; Global buckling.

1. Introduction

The strength of cold-formed steel (CFS) compression members is governed by local buckling, distortional buckling, global buckling, and their interactions before gross-section yielding. The effective width method (EWM) and the direct strength method (DSM) are two major design philosophies used in the strength evaluation of these members. These two design methods are now part of AISI S100 [1] and AS/NZS 4600 [2] design provisions. DSM has been thoroughly investigated, and appropriate modifications have been suggested for CFS members' cross-sectional buckling behaviour [3-5]. But for global buckling, limited studies are reported in the literature [6-9]. Sometimes, the global buckling strengths of CFS members are evaluated by the design equations of hot-rolled steel members (AISC-360 [10]); one such example is the expression for the design for built-up sections as given in AISI S100 [1].

Built-up CFS sections are gaining popularity in the construction of low- to mid-rise buildings due to their simple fabrication process and improved axial and flexural rigidity compared to single CFS sections. These built-up sections can be formed by connecting single sections in different arrangements such as back-to-back connected I-shape [11] or face-to-face connected box-shape [12]. Self-drilling, self-tapping screws or plug welds are generally used at suitable intervals in these connections. The global buckling (minor axis buckling) strength is evaluated by modifying the slenderness ratio (Eq. 1) of built-up members, as suggested in AISI S100 [1]. Although this modification is developed for hot-rolled steel members [10], it has also been extended to cold-formed steel members. The modified slenderness ratio (MSR) as given in AISI S100 [1] is,

$$\left(\frac{KL}{r}\right)_m = \sqrt{\left(\frac{KL}{r}\right)_0^2 + \left(\frac{s}{r_i}\right)^2} \tag{1}$$

in which $(KL/r)_0$ is the fully-composite slenderness ratio of the built-up section; s is the fastener spacing; r_i is the minimum radius of gyration of the full unreduced cross-sectional area of the single section. The effect of using MSR on the ultimate strength of CFS built-up columns was evaluated by Stone and LaBoube [13]. Using the test results of back-to-back connected lipped channel sections, they showed that the use of MSR would result in conservative strength predictions (up to 60%) for sections with thickness more than 0.89 mm. In addition to the MSR, AISI S100 [1] suggests using closely spaced fasteners near the supports to reduce the relative displacement or shear slip between joined sections. The effect of end fastener groups (EFGs) on built-up columns' buckling behaviour was investigated experimentally by Fratamico et al.

[11]. They found that the ultimate strength in flexural buckling can increase by up to 40% when EFGs are used.

The nominal global buckling strength (P_{ng}) of CFS members as per DSM is a function of non-dimensional slenderness ratio (λ_g) alone, which is the square root of the ratio of yield load (P_y) and elastic critical global buckling load (P_{crg}) of the member. The global buckling load of single sections can be computed through either Euler's buckling formula for flexural buckling or flexural-torsional buckling formula [1]. For cross-sectional buckling loads, such as for local buckling and distortional buckling, a computational tool CUFSM [14] is used. For built-up sections, the fasteners will enable a partial-composite buckling behaviour in flexural buckling mode. Hence, the critical global buckling load will be more than the P_{crg} of a single section but less than the P_{crg} of the fully-composite section (section with the total thickness of connecting sections).

In the literature, the buckling stress of built-up sections was calculated approximately by Young and Chen [15] for built-up box-sections and Zhang and Young [16] for built-up I-sections by developing different models using CUFSM. They used the buckling stress results with DSM design equations and proposed design procedures for the built-up section columns. Fratamico et al. [17] developed a framework with a semi-analytical fastener element and investigated the sensitivity of flexural buckling behaviour of built-up sections with the effect of fastener shear stiffness. To compute the actual elastic critical buckling stress of built-up sections with discrete fasteners, Abbasi et al. [18] developed a finite strip-based computational tool using a compound methodology developed by Puckett and Wiseman [19] wherein the stiffness of fasteners is added into the finite strip framework. This tool can be used to analyse different types of built-up sections, but it contains limitations of the finite strip method. An analytical equation for computing the global buckling stress of back-to-back connected built-up I-sections with discrete fasteners was presented by Zhou et al. [20]. Rasmussen et al. [21] suggested an analytical method for assessing the effective flexural rigidity (EI_{eff}) by incorporating the shear flexibility at discrete fastener locations in built-up sections. They showed that the built-up section's effective rigidity in flexural buckling varies between different fastener locations, and its value depends on the fastener spacing.

The literature review presented above shows that significant research has been performed on computing the ultimate strength of built-up CFS columns. But in the context of computing the critical buckling stress of built-up sections, only a few studies have been presented

[17,18,20,21]. As pointed out earlier, the modified slenderness ratio produces conservative ultimate strength predictions Hence, the modified slenderness ratio equation needs to be assessed with the slenderness ratio computed using the actual global buckling stress of built-up columns. The modified slenderness ratio as per AISI S100 [1] is applicable when two sections are in contact, and the buckling deformation will produce a shear force in the connectors, which is true for back-to-back connected built-up sections under uniform compression.

This study will assess the constitutive elements of the modified slenderness ratio and their applicability to the true prediction of the flexural buckling behaviour of the built-up CFS columns. The actual critical buckling stress of built-up columns is computed by developing a numerical framework using the compound spline finite strip method (CoSFSM) developed by Mahar and Jayachandran [22]. Also, specially developed mode-specific constraints were applied to the numerical model of the built-up sections to produce the flexural buckling mode. An equivalent slenderness ratio was computed from the results of the buckling analysis of the CoSFSM framework, which was then compared with the modified slenderness ratio predictions. A total of 228 experimental and numerical results (including 16 results of built-up sections with EFGs) of back-to-back connected built-up sections [11,13,16,20,23-26] published in the literature were investigated. The results were used to assess the relative accuracy of different design standards with buckling stress computed through different frameworks, i.e., spline finite strip, modified slenderness ratio, fully-composite section slenderness ratio, etc. Based on the assessment, a compound slenderness ratio (CSR) is proposed, verified using the results obtained from the literature. This study focuses on the minor axis buckling of back-to-back connected built-up sections, which is generally the critical mode of buckling. Hence, the term global buckling will be used in this study with reference to the minor axis buckling.

2. Studies on the modified slenderness ratio

The presence of discrete connections in a built-up section will develop a partial-composite global buckling behaviour due to the occurrence of shear slip in the unconnected regions [21]. This discontinuity present in the built-up member's unconnected region will reduce the ultimate strength. This effect is captured by increasing the global slenderness in terms of modified slenderness ratio (Eq. 1). This equation was first introduced in the AISC-LRFD design manual [27], based on Zandonini's [28] experimental study of back-to-back connected channel sections with 20 mm filler plates and snug-tight bolts. The experimental results of Zandonini [28] for

channel sections and those of Astaneh et al. [29] for double angle sections were studied by Duan and Chen [30]. They suggested that the snug-tight bolts will behave as pinned-end for the shear effect in the unconnected region. Thus, shear slip is an important parameter affecting the flexural deformations in back-to-back connected sections, and it may reduce the ultimate strength in global buckling.

In the context of CFS built-up sections, the connections are generally formed by self-tapping screws. These connections experience shear during flexural deformations, and in result, the tilting of screws is generally observed. This may lead to excessive relative displacement [11], and the built-up CFS section will move away from the fully-composite buckling behaviour towards a partial-composite buckling behaviour. Thus, the interaction between shear slip and flexural deformation can directly influence built-up CFS members' ultimate strength.

The built-up sections used in studies of Zandonini [28] and Astaneh et al. [29] will experience less shear slip than CFS sections. The major factors can be a comparatively high projected area for shear resistance (screw/bolt diameter), the use of filler plates and the absence of tilting of screws. The modified slenderness ratio does not include any term representing the interaction between shear slip and flexural buckling. This formulation yielded good results for hot-rolled steel built-up members as there was less interaction due to low shear slip. As the shear slip interacts more with the flexural deformations (specimens with high fastener spacing), the modified slenderness ratio will increase excessively as the term (s/r_i) will dominate. It may produce conservative strength predictions for CFS built-up sections, especially in high fastener spacing regions. Thus, MSR's global buckling stress predictions need to be compared with the actual buckling stress solutions. The increment in the slenderness ratio of built-up columns with respect to the fully-composite section's slenderness ratio can be presented by a factor 'α' as shown in Eq. (2). An expression for α representing the modified slenderness ratio (MSR) (Eq. 3) can be derived from Eq. (2).

$$\text{Modified slenderness ratio } \left(\frac{KL}{r}\right)_m = \sqrt{\left(\frac{KL}{r}\right)_0^2 + \left(\frac{s}{r_i}\right)^2} = \alpha \times \left(\frac{KL}{r}\right)_o \tag{2}$$

$$\alpha\ (MSR) = \sqrt{1 + \left(\frac{s}{KL}\right)^2 \left(1 + \left(\frac{x}{r_i}\right)^2\right)} \tag{3}$$

where, x is the distance between the minor axes of built-up and single sections. The factor 'α' is the partial-composite factor of the built-up column, representing the effect of shear slip in terms of fastener spacing and cross-sectional geometry.

In Section I1.2 of AISI S100 [1], along with the modified slenderness ratio, additional fastener grouping at the ends and fastener spacing conditions are also specified to reduce the excessive shear slip. The effect of these specifications on the strength prediction of built-up columns using a modified slenderness ratio needs to be verified. To understand the partial-composite behaviour of built-up sections, the effect of shear slip in terms of buckling stress computed from the actual buckling stress solutions of a proposed framework was compared with the modified slenderness ratio predictions. Then the effect of fastener spacing conditions suggested in AISI S100 [1] on ultimate strength was investigated.

3. Compound spline finite strip method (CoSFSM)

The computation of elastic critical buckling stress of a folded plate system using the spline finite strip method has been discussed in the literature [31-33]. For a built-up section, in addition to the energy formulations for thin plates, strain energy of fastener elements needs to be added to the total system's strain energy [19,34]. This is achieved by considering the fasteners as three-dimensional beam elements and by an appropriate transformation of axes and then correlating the beam displacements with displacements of plate strips [18]. The fastener cross-section was assumed to be circular with a diameter of 4.8 mm [18, 24]. The fastener material properties (Young's modulus, E = 203,000 MPa and Poisson's ratio = 0.3) were selected based on AISI S100 [1]. A typical diagram of an arbitrary oriented beam element connected to two strips is shown in Fig. 1 with each individual system's local axis.

Fig. 1. Compound system of beam element and plate strips with strip orientations in the global coordinate system.

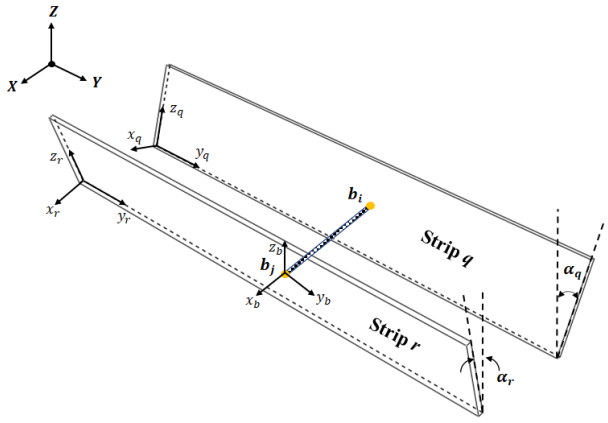

The total strain energy for the compound system shown in Fig. 1, can be written as,

$$\Pi = \Pi_i + \Pi_j + \sum_{k=1}^{NF} \Pi_k \tag{4}$$

in which Π_i, Π_j are the strain energy of *i*-th and *j*-th strip, *NF* is the total number of fasteners and Π_k is the strain energy of *k*-th fastener. The strain energy of the beam element (Π_b) in global spline finite strip system (SFS) can be written as,

$$\Pi_b = \frac{1}{2} \{\delta_p^G\}^T [K_b^{SFS}] \{\delta_p^G\} \tag{5}$$

in which $\{\delta_p^G\}$ is the plate strip's displacement vector, and $[K_b^{SFS}]$ is the stiffness matrix of fastener element transformed into spline finite strip system and is given in Eq. (6).

$$[K_b^{SFS}] = [T]^T [T_c]^T [R_{GL}]^T [R]^T [K_b^L] [R] [R_{GL}] [T_c] [T] \tag{6}$$

The detailed formulations of CoSFSM are presented in Mahar and Jayachandran [22] where the boundary conditions were enforced using spline amendment scheme suggested by Ajeesh and Jayachandran [35]. The buckling analysis can be performed by solving the generalised Eigenvalue problem given in Eq. (7). The Eigenvalues (λ_i) and respective Eigenvectors ($\boldsymbol{X_i}$) are then used to determine the different buckling modes. The Eigenvalue equation will be as shown in Eq. (7).

$$[A]\boldsymbol{X} = \lambda [B]\boldsymbol{X} \tag{7}$$

$$[A] = [K] + \sum_{i=1}^{NF} [K_i^{SFS}] \tag{8}$$

$$[B] = [K_G] \tag{9}$$

where, $[A]$ is the global stiffness matrix and $[B]$ is the global geometric stiffness matrix of the compound system.

3.1. Mode specific constrained models

The buckling stress computed using the CoSFSM [22] will not explicitly represent the pure buckling modes, as the use of spline functions in the longitudinal direction can produce mixed buckling modes. Hence, mode-specific constraints were developed to capture the buckling behaviour in a specific buckling mode based on the particular mode's deformation profile [36]. In this study, a specific constraint model was developed to allow only the minor axis buckling deformation in buckling analysis and effectively constrain other buckling modes. The constraint model for a single section is shown in Fig. 2, and these constraints will be applied to the node line throughout the length of the member. These models were then extended to the back-to-back built-up sections, and the critical buckling stress for minor axis buckling mode was computed. The limitation of these models is that the local buckling deformations may appear if local buckling is the critical buckling mode. Still, the deformed shape can identify the

global buckling mode in higher buckling modes. These models can effectively restrict distortional, flexural-torsional, and torsional buckling mode in the buckling analysis.

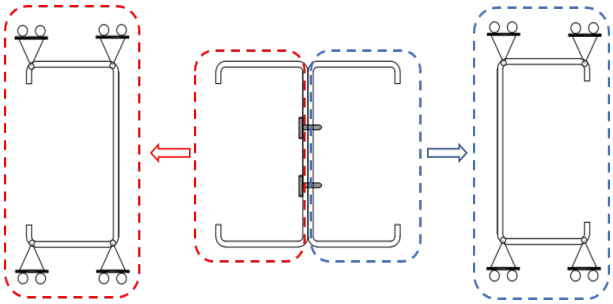

Fig. 2. Constrained models to allow minor axis buckling mode

3.2. Validation of CoSFSM constrained models

The partial-composite global buckling behaviour in back-to-back connected lipped channel sections was investigated by Zhou et al. [20] who developed an analytical formula to calculate the minor axis flexural buckling stress. The global buckling stress results of constrained models (Fig. 2) were compared with Zhou et al.'s [20] 42 back-to-back connected lipped channel sections with the help of finite element (FE) study. The FE model was developed in ABAQUS [37] based on the suggestions of Abbasi et al. [18] where channels were modelled with S4R elements and fasteners were modelled as three-dimensional wire (B3) elements. The mesh size of 10 mm × 10 mm was selected, and an Eigenvalue analysis was performed to calculate the global buckling stress of the built-up I section. The proposed constrained model results were found to be in good agreement with the FE results (Fig. 3) as the mean ratio of the CoSFSM results to FE results were 0.982 with a CoV of 0.016.

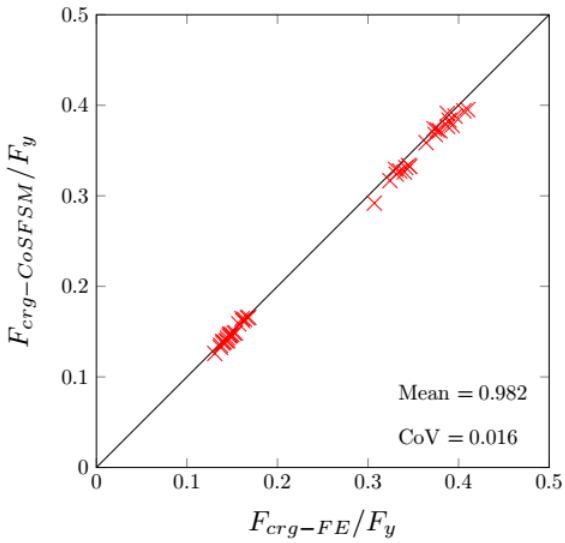

Fig. 3. Comparison of global buckling stresses (F_{crg}) from the constrained model of CoSFSM [22] ($F_{crg\text{-}CoSFSM}$) and FE results ($F_{crg\text{-}FE}$)

After verifying the constrained model results, the proposed CoSFSM framework with constrained models was extended to 228 specimens. Generally, the fastener spacing in slender columns is greater than the local buckling half-wavelength but even for the small fastener spacing, the gain in local buckling strength will be negligible. The effect of fastener spacing on local buckling behaviour was studied by Mahar and Jayachandran [22]. As per their suggestions, the critical local buckling stress of built-up sections, F_{cr} (LB), can be assumed to be equivalent to that of its single section [22]. In this study, the critical local buckling stress results obtained using CUFSM were used for the analysis.

4. Investigation of shear slip behaviour

The partial-composite factor (α) can be set as a quantification unit for the shear slip, which will show the appropriate increment required in the slenderness from that of a fully-composite section. For this, 42 numerical results from Zhou et al. [20] on different fastener spacing were used as the basis. The formulations for different partial-composite factors (α) are provided in Table 1, where α is the ratio of the slenderness ratio of built-up section (calculated using different methods) and the slenderness ratio of fully-composite section.

Table 1. Formulations for partial-composite factor (α)

Slenderness ratio (SR)	Formula	$\alpha = \frac{SR}{FcSR}$
Slenderness ratio of fully-composite section (FcSR)	$\left(\frac{KL}{r}\right)_o$	1
Modified slenderness ratio (MSR) (AISI 2016)	$\left(\frac{KL}{r}\right)_{AISI} = \sqrt{\left(\frac{KL}{r}\right)_0^2 + \left(\frac{s}{r_i}\right)^2}$	$\frac{(KL/r)_{AISI}}{(KL/r)_o}$
Slenderness ratio as per CoSFSM	$\left(\frac{KL}{r}\right)_{CoSFSM} = \sqrt{\frac{\pi^2 E}{F_{cr}(GB)_{CoSFSM}}}$	$\frac{(KL/r)_{CoSFSM}}{(KL/r)_o}$
Slenderness ratio as per Zhou et al. [20]	$\left(\frac{KL}{r}\right)_{Zhou} = \sqrt{\frac{\pi^2 E}{F_{cr}(GB)_{Zhou}}}$	$\frac{(KL/r)_{Zhou}}{(KL/r)_o}$

Fig. 4 shows that the modified slenderness ratio results match well with the results of Zhou et al. [20] when the fastener spacing is small ($s \leq L/5$). These specimens will behave as fully-composite sections since the values of 'α' for these specimens are closer to one. But as the fastener spacing increases, the effect of shear slip predicted by the modified slenderness ratio

does not reflect the actual behaviour, and the difference can be about 20% for some fastener spacings. Thus, the shear slip behaviour predicted by the MSR will be higher than actual and the impact of such variations on the ultimate global buckling strength need to be explored.

In the next section, the constituent elements of the modified slenderness ratio are studied to understand the applicability of existing formulation (MSR) for the strength prediction of built-up CFS columns.

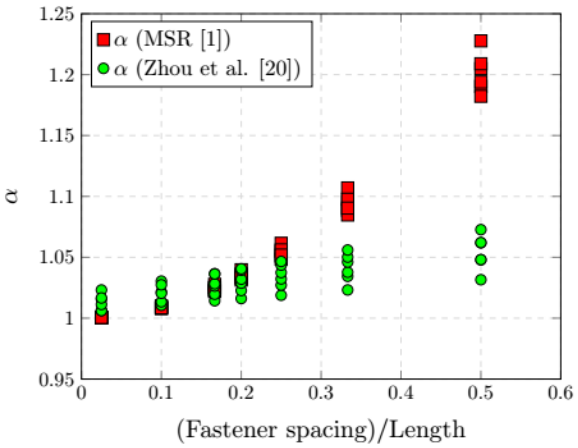

Fig. 4. Variation of partial-composite factor 'α' with different fastener spacings

5. Evaluation of global buckling strength

In this study, 212 experimental and numerical results (excluding 16 specimens with end fastener groups) of globally buckling built-up CFS columns from the literature were used for the analysis. All the data are presented in Tables A1 to A6 of the Appendix. In repeated experimental results, the average value of the results was used in this study. The modulus of elasticity was considered 203 GPa [1] with Poisson's ratio of 0.3. The critical global buckling stress was computed by three methods, i) CoSFSM with constrained models (Fig. 2), ii) by using modified slenderness method, and iii) by using fully-composite section properties (fully-composite slenderness ratio). All the results were checked for possible interaction with local buckling. The local-global buckling interaction was avoided by keeping the elastic critical local buckling load (P_{crl}) to be at least 1.66 times more than the ultimate strength (P_u) of the member [36]. This limit is calculated from DSM equations [1], which indicates that if the P_{crl}/P_u value is less than 1.66 ($\lambda_l = \sqrt{P_u/P_{crl}} > 0.776$), local-global interaction may occur. Thirty-eight specimens were influenced by local buckling as per the above criterion and were not considered here.

5.1. Assessment of design standards

AISI S100 [1] suggests both effective width method (EWM) and direct strength method (DSM) for the design of globally buckling built-up compression members with the use of modified slenderness ratio. Eurocode (EN: 1993-1-3) [38] suggests the EWM, and for different built-up formations, different buckling classes are given for imperfections. To compare the design strength predictions with the test and numerical results obtained from literature, it becomes important to calculate the actual buckling stress of partially-composite built-up members subjected to global buckling. This was achieved by developing models with mode-specific deformations in the compound spline finite strip-based framework for the specimens considered in this study. The buckling stress results (F_{cr}) are presented in Tables A1 to A6 of the Appendix.

5.1.1. Global slenderness ratio predictions

The critical global buckling stress computed using the proposed framework with constrained models was used to calculate the 'equivalent' slenderness ratio of the specimens. The modified slenderness ratio (MSR) $(KL/r)_m$ and the equivalent slenderness ratio from the present study was then compared with the fully-composite slenderness ratios (FcSR) $(KL/r)_o$ in terms of the partial-composite factor (α). The observations are presented under three groups based on the normalised fastener spacing ratio (sr_o/KLr_i) and these results are plotted in Fig. 5. The normalisation factor was selected such that the effect of geometry and fastener spacing can be captured as α is a function of both parameters.

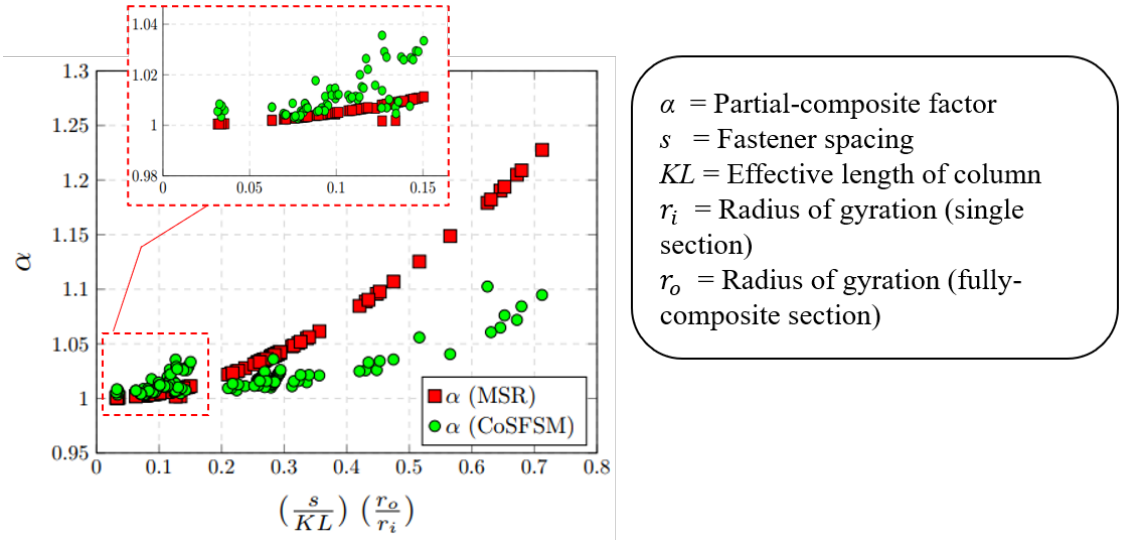

Fig. 5. Variation of partial-composite factor (α) with normalised fastener spacing

As per the study on slenderness ratio (Fig. 5), when the fastener spacing is relatively low ($sr_o/KLr_i < 0.2$), the modified slenderness ratio will be closer to fully-composite slenderness ratio as the $(s/r_i)^2$ component will be very small compared to the fully-composite slenderness ratio $(KL/r)_o$. In the high fastener spacing region ($sr_o/KLr_i > 0.33$), where the shear slip is expected to interact with flexural buckling, the modified slenderness ratio predictions will be very high compared to the equivalent slenderness ratio. These data points contain the results for both pin-ended and fixed-ended columns, and the obtained behaviour is found to be similar for both support conditions. For a better representation of the contribution of each component of Eq. (1), a surface plot is presented in Fig. 6 with the slenderness ratio values obtained from 174 results. The plot shows that with an increase in fastener spacing, the MSR will move away from the actual behaviour. The increment in slenderness is too rapid, and the difference becomes relatively large for high fastener spacing. The effect of such variations in slenderness ratio values on the ultimate strength prediction is presented next.

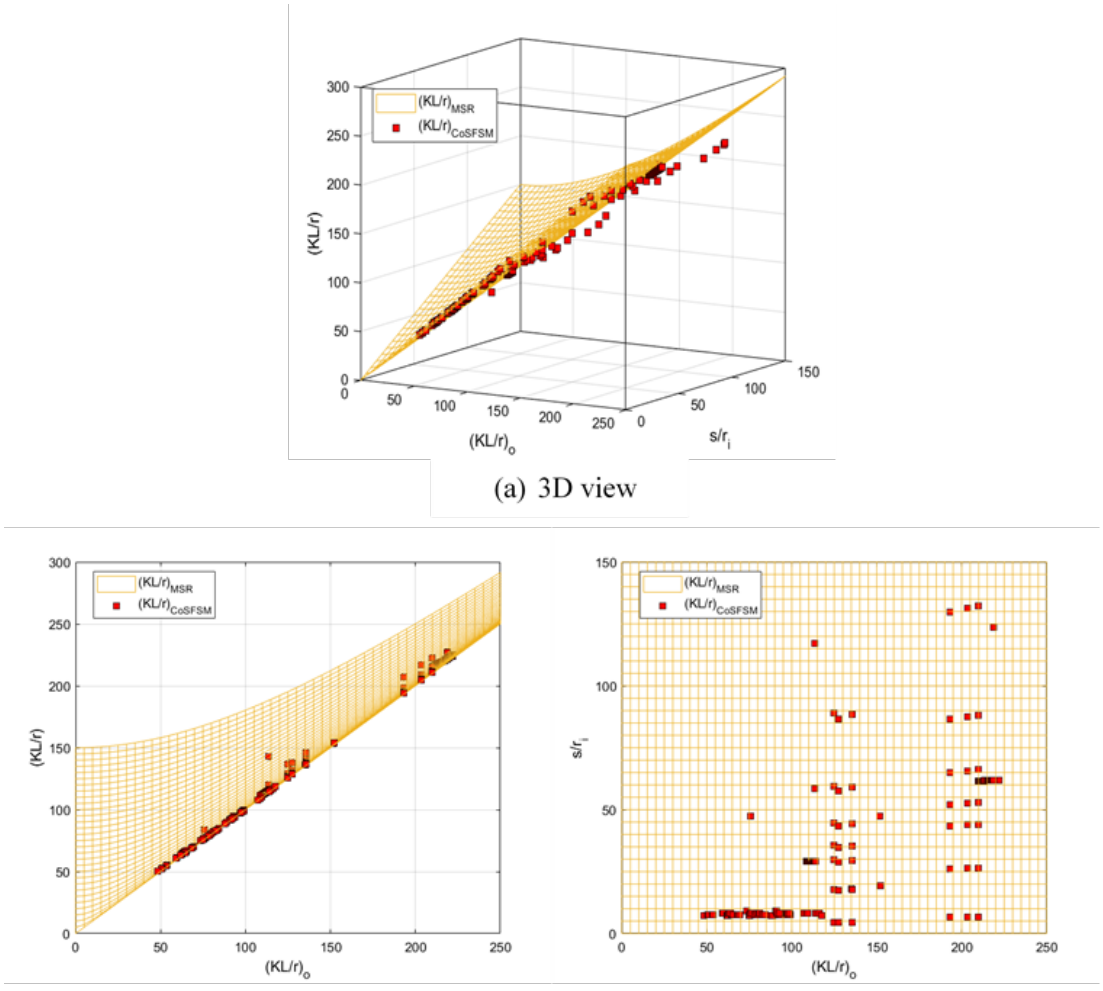

Fig. 6. Surface plot of modified slenderness ratio (AISI) and comparison with equivalent slenderness ratio (CoSFSM) values.

5.1.2. Global buckling strength prediction

In this section, the buckling stress results obtained using CoSFSM and those from MSR were used in the different design framework (DSM, EWM) to compute the nominal global buckling strength (P_{ng}). All the 174 results (excluding 38 results of local-global interaction) of global buckling strength predictions (P_{ng}) were compared with the corresponding test/numerical results (P_u), and the average values of P_u/P_{ng} are presented in Table 2. The comparison study shows that the AISI-DSM [1] design strength prediction using MSR will be appropriate for low fastener spacing regions ($sr_o/KLr_i \leq 0.2$) but are highly conservative for higher fastener spacing regions. The AISI-EWM [1] strength predictions are generally conservative in all spacing regions while Eurocode [38] predictions are unconservative in high spacing regions ($sr_o/KLr_i > 0.33$). The strength predictions using Eurocode [38] were unconservative as the design equations do not account for the fastener spacing and are a function of the buckling behaviour of fully-composite section alone.

The study on slenderness ratio and the ultimate strength prediction shows that the modification in slenderness ratio directly impacts the ultimate strength of built-up columns. The use of MSR in the higher fastener spacing range ($sr_o/KLr_i > 0.2$) will predict conservative strength, and for the lower fastener spacing range, the effect of the modification is not significant. The strength predictions using the buckling stress results of CoSFSM constrained model with DSM are in good agreement with the test/numerical results. Thus, the DSM global buckling strength equations are appropriate for design if actual buckling stress values of the built-up sections are used for the strength predictions. In the next section, a compound slenderness ratio (CSR) is proposed to alleviate the issues related to MSR for built-up back-to-back connected columns, which is verified using the buckling stress results of the CoSFSM framework.

Table 2. Design global buckling strength predictions for different fastener spacing ranges

Fastener spacing range	Number of specimens	Mean value of P_u/P_{ng} ratio				
		DSM (SR-CoSFSM)	AISI-DSM (MSR)	AISI-EWM (MSR)	Eurocode (FcSR)	AISI-DSM (CSR)
$(sr_o/KLr_i) \leq 0.20$	70	1.009	1.00	1.006	1.101	1.00
$0.2 < (sr_o/KLr_i) \leq 0.33$	84	1.006	1.044	1.054	1.002	1.024
$(sr_o/KLr_i) > 0.33$	20	0.981	1.164	1.175	0.934	0.960
Total specimens = 174	Mean	1.003	1.040	1.048	1.033	1.010
	CoV	0.108	0.127	0.125	0.116	0.108

5.2. Compound slenderness ratio (CSR)

The observations from Figs. 5 and 6 show that the smaller fastener spacing region is less sensitive while, the higher fastener spacing region is highly sensitive to the modified slenderness ratio. This is because the shear slip interaction effect is not reflected in the formulation. The effect of shear slip can be observed in the higher fastener spacing region ($sr_o/KLr_i > 0.2$), where the modified slenderness ratio predicts excessively conservative strength predictions. A compound slenderness ratio is therefore suggested in Eq. (10) to represent a better interaction between local slenderness of unconnected region (s/r_i) and overall slenderness of the member $(KL/r)_o$ in all fastener spacing regions. All the terms have similar meanings as given in Eq. (1). The factor of 0.2 was calculated by performing a statistical study based on comparing the predictions of CSR with the global buckling load results (P_{crg}) from CoSFSM. The CSR based buckling stress predictions were found to be in good agreement with CoSFSM based buckling stress results of 174 specimens (Fig. 7), as the mean ratio was 1.002 with CoV of 0.016.

$$\text{Compound slenderness ratio (CSR)} \left(\frac{KL}{r}\right)_{CSR} = \sqrt{\left(\frac{KL}{r}\right)_0^2 + \frac{s}{r_i} \times 0.2 \left(\frac{KL}{r}\right)_o} \tag{10}$$

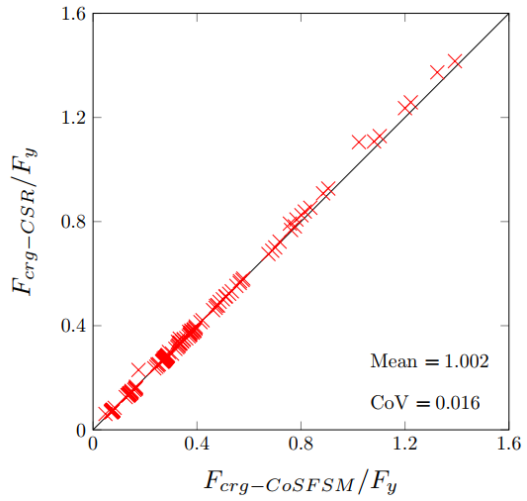

Fig. 7. Comparison of global buckling stress (F_{crg}) from the proposed CSR ($F_{crg\text{-}CSR}$) and constrained model of CoSFSM [22] ($F_{crg\text{-}CoSFSM}$)

In Fig. 8, the proposed CSR formulation is plotted against the normalised fastener spacing ratio, which shows a good relationship with the actual partial-composite buckling behaviour in terms of α. A better representation of the CSR variation with each component is presented in Fig. 9,

which shows that the proposed formulation will effectively capture the shear slip effect with change in local slenderness of unconnected region.

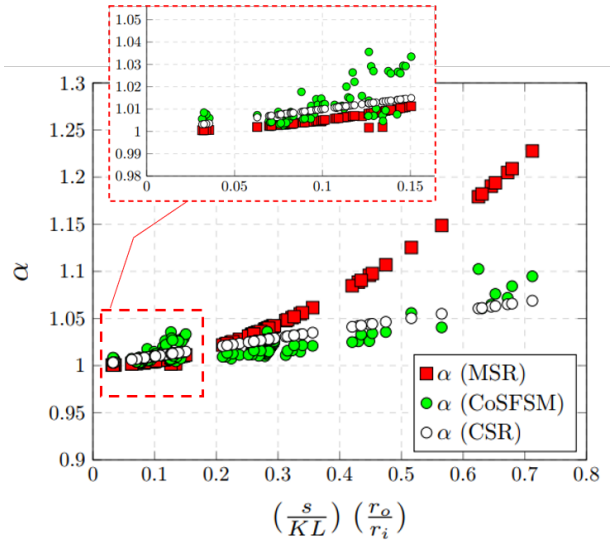

Fig. 8. Comparison of proposed compound slenderness ratio (CSR) with other slenderness ratios (MSR, CoSFSM) against normalised fastener spacing

The ultimate global buckling strength prediction using DSM equations with the proposed slenderness ratio (CSR) shows better results than existing MSR, as the mean value is close to one. A comparison is presented in Fig. 10 between the strength predictions using existing MSR and proposed CSR with DSM design equation against the normalized ratio of fastener spacing and length of the column. The comparison shows that the proposed CSR will show better strength predictions than MSR in low and high spacing regions. Table 4 shows the results of a statistical study for ultimate strength predictions by different design standards.

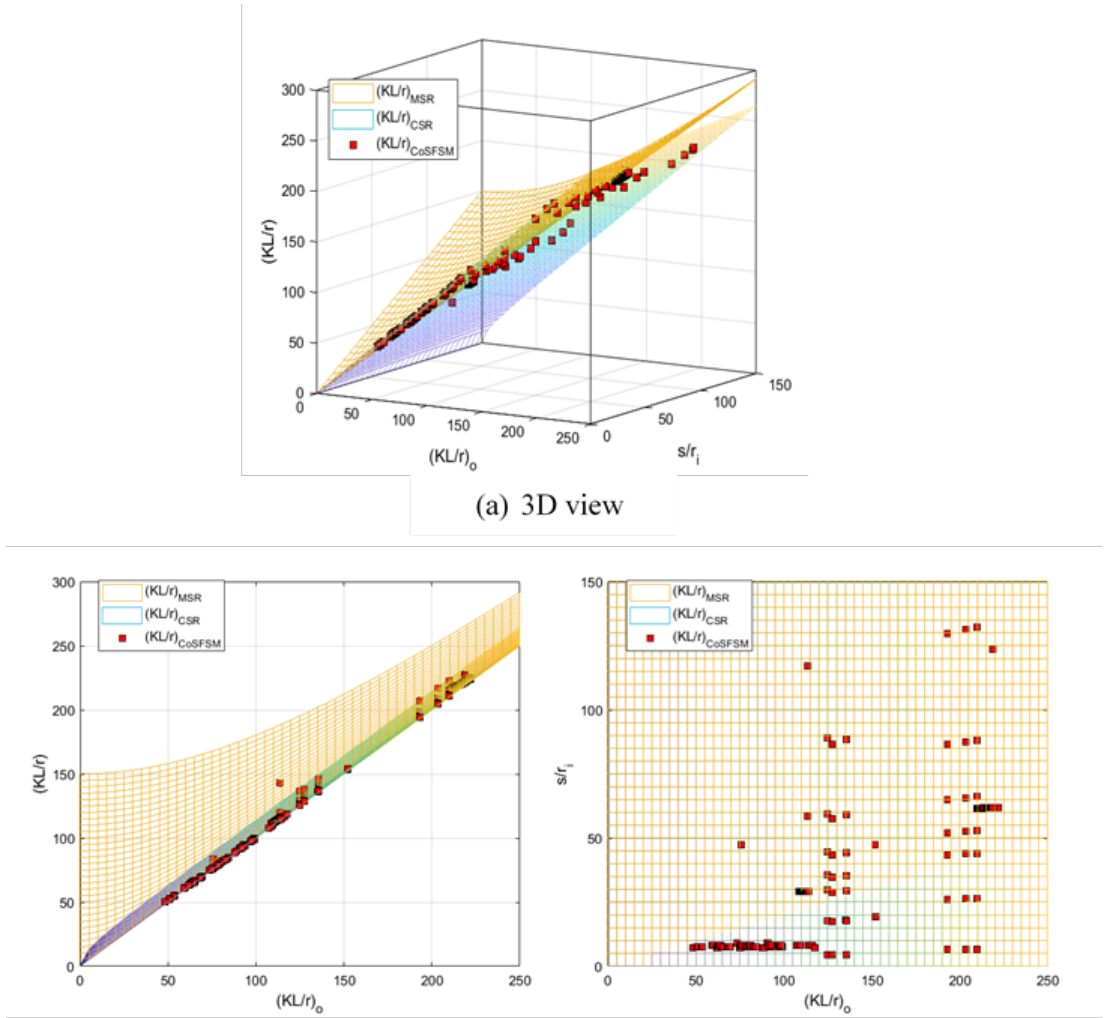

Fig. 9. Surface plot of proposed slenderness ratio (CSR) and modified slenderness ratio (MSR) with comparison to equivalent slenderness ratio values

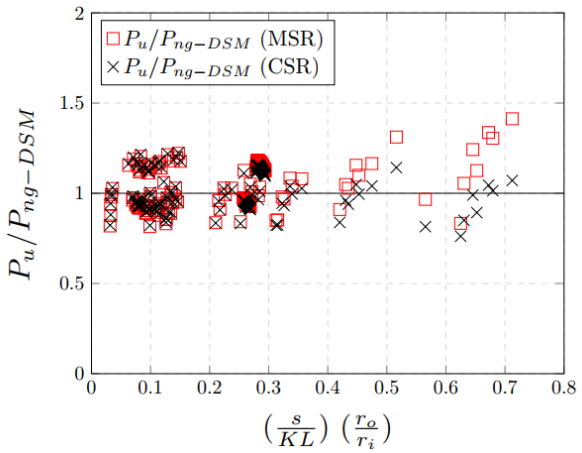

Fig. 10. Global buckling strength predictions of DSM using MSR and CSR against fastener spacing

6. Effect of end fastener group (EFG)

As per Section I1.2 of AISI S100 [1], additional end fastener group at both ends of the column shall be attached up to 1.5 times the section width. This recommendation will help in reducing the excessive shear slip in built-up columns. Although AISI S100 [1] recommends EFGs, its effect is not reflected in the modified slenderness ratio formulation. In the previous section, the AISI S100 [1] global buckling strength predictions using the modified slenderness ratio were found to be conservative, and with the application of EFGs, the strength predictions will become over-conservative.

Table 3. Strength predictions using CoSFSM, MSR and CSR for built-up columns with EFGs (Fratamico et al. [11])

Specimen	F_{cr} (GB) (MPa)	$\frac{P_{u,Test}}{P_y}$	DSM (CoSFSM) $\frac{P_u}{P_{nlg,CoSFSM}}$	AISI (DSM) $\frac{P_u}{P_{nlg,MSR}}$	AISI (EWM) $\frac{P_u}{P_{nlg,MSR}}$	DSM (Proposed CSR) $\frac{P_u}{P_{nlg,CSR}}$
A1-250S137-33	608.40	0.57	0.964	1.136	1.079	1.098
A1-250S1374	640.94	0.61	0.878	1.053	1.101	1.016
A1-250S134	629.61	0.71	0.942	1.263	1.312	1.186
A1-250S137-68	608.70	0.67	0.839	1.110	1.110	1.049
B1-362S137-33	581.37	0.45	0.976	1.144	0.987	1.111
B1-362S137-43	611.52	0.54	0.972	1.157	1.100	1.122
B1-362S137-54	647.47	0.53	0.877	1.096	1.113	1.056
B1-362S137-68	668.87	0.54	0.708	0.893	0.965	0.849
C1-600S137-33	451.44	0.38	1.238	1.522	1.241	1.475
C1-600S137-43	459.33	0.44	1.206	1.327	1.150	1.295
C1-600S137-54	442.74	0.39	1.003	1.117	1.029	1.085
C1-600S137-68	446.70	0.52	1.040	1.153	1.143	1.123
D1-600S162-33	681.03	0.35	1.043	1.180	0.950	1.155
D1-600S162-43	684.90	0.37	0.933	1.062	0.900	1.039
D1-600S162-54	696.75	0.49	1.127	1.321	1.177	1.287
D1-600S162-68	688.06	0.55	1.017	1.177	1.147	1.149
		Mean	0.985	1.170	1.094	1.131
		CoV	0.136	0.120	0.099	0.123

The actual buckling stress results of CoSFSM and the proposed formulation of compound slenderness ratio (CSR) were investigated to compare the strength predictions using MSR for the built-up sections with EFGs. The CoSFSM can incorporate the EFGs in the numerical

model and the actual buckling stress of such sections can be computed. All the results are presented in Table 3. Since the specimens failed in local-global interaction, the local buckling stresses of these sections were calculated using the single section model in CUFSM. As expected, the design strength predictions with MSR ($P_{nlg,MSR}$) were found to be conservative by 17% and 9.4%, for DSM and EWM, respectively. The DSM design predictions with actual buckling stress results of CoSFSM matches well with the test results. The DSM formulations with the proposed CSR for local-global bucking interaction ($P_{nlg,CSR}$) were conservative by 13.1%. The design predictions using both MSR and CSR are conservative as the effects of EFGs are not included in the formulation of slenderness ratio, and shear slip is always expected. The average increment in the strength of built-up sections with EFGs was 12.6% from the strength of sections without EFGs [11]. Hence, if the effect of EFGs is added to the global buckling strength predictions then the CSR may predict the strength appropriately.

7. Reliability analysis

The reliability of DSM based design results computed using the proposed slenderness ratio is checked using Eq. (11) as per AISI S100 [1] for LRFD.

$$\beta_o = \frac{-\ln\left[\frac{\phi}{1.52\, M_m F_m P_m}\right]}{\sqrt{{V_m}^2+{V_f}^2+C_p{V_p}^2+{V_q}^2}} \tag{11}$$

The capacity reduction factor (ϕ) for columns is 0.85, the mean value of material factor (M_m) is 1.10, the mean value of fabrication factor (F_m) is 1.0, the CoV of material factor (V_m) is 0.1, the CoV of fabrication factor (V_f) is 0.05, and the CoV of load effect (V_q) is 0.21. P_m and V_p are the mean and CoV values of the ratio of the test/numerical results to the predicted results from the proposed equation. The value of C_p can be obtained from Eq. (12).

$$C_p = \left(1 + \frac{1}{n}\right)\left(\frac{m}{m-2}\right) \tag{12}$$

where, n = numbers of test/numerical results 174 and m is the number of degrees of freedom = (n-1). The target reliability as per AISI S100 [1] for LRFD is 2.5. The reliability of the proposed equation (CSR) with DSM design equation is 2.62, which is higher than the target reliability. The reliability of MSR with DSM design equation is 2.65. The capacity reduction factor (ϕ) for the target reliability (β_o=2.5) is found to be 0.87 for the strength prediction using the proposed equation (CSR), and 0.89 for the existing equation (MSR). The results are presented in Table 4.

Table 4. Values of coefficients (P_m, V_p) and reliability index (ϕ, β_o) for proposed and existing equations for global buckling

	(P_u/P_{ng})				
	CoSFSM-DSM	MSR-DSM	MSR-EWM	FcSR-Eurocode	CSR-DSM
	$\left(\frac{P_u}{P_{ng,CoSFSM}}\right)_{DSM}$	$\left(\frac{P_u}{P_{ng,MSR}}\right)_{DSM}$	$\left(\frac{P_u}{P_{ng,MSR}}\right)_{EWM}$	$\left(\frac{P_u}{P_{ng,FcSR}}\right)_{EC3}$	$\left(\frac{P_u}{P_{ng,CSR}}\right)_{DSM}$
n	174	174	174	174	174
P_m	1.004	1.041	1.049	1.034	1.010
V_p	0.108	0.127	0.125	0.116	0.108
$\beta_o(\phi = 0.85)$	2.602	2.650	2.691	2.678	2.623
ϕ (β_o= 2.5)	0.873	0.885	0.895	0.891	0.878

8. Summary and conclusions

The present study evaluated the design recommendations of Section I1.2 of AISI S100 [1] for cold-formed steel built-up columns connected discretely with screw fasteners. For this evaluation, a compound spline finite strip-based numerical framework developed by the authors and 228 experimental and numerical results published in the literature were used as the basis. First, the actual global buckling stress of built-up columns was evaluated by developing models with mode-specific deformations in compound spline finite strip framework. The proposed models were validated using the FE modelling results. The buckling stress results of AISI S100 [1] based on the modified slenderness ratio (MSR) were compared with the results of compound spline finite strip-based numerical model, and the shortcomings of MSR predictions (overly conservative) were highlighted for the high fastener spacing range.

The modified slenderness ratio was shown to be applicable only for low fastener spacing region ($sr_o/KLr_i \leq 0.2$). For high fastener spacings, the shear slip between the individual sections of a built-up column and its interaction with flexural buckling dominates the strength and MSR neglects this interaction. A compound slenderness ratio (CSR) was thus proposed, which can predict the ultimate global buckling strength predictions well for all fastener spacings in comparison with the experimental and numerical results presented in the literature. This study has shown that the reliability of the DSM design equations with the proposed CSR is higher than the target reliability (β_o = 2.5) of AISI S100 [1] for LRFD. The effect of end fastener group (EFG) on the global buckling strength was also investigated, and the DSM formulations

with the proposed CSR gave improved strength predictions compared to the MSR in AISI S100 [1].

Appendix A

Test and numerical results (P_u) of the built-up cold-formed steel columns published in the literature (Stone and LaBoube [13]; Zhang and Young [16,24]; Craveiro et al. [25]; Lu et al. [26]; Roy et al. [23]; Zhou et al. [20]; Fratamico et al. [11]) were analysed and the results are presented next.

Table A1. Analysis of back-to-back channel sections used in Stone and LaBoube [13] with global buckling stress (F_{crg}) computed using CoSFSM framework

Specimen	$\frac{s}{KL}$	F_y (MPa)	P_u (kN)	F_{crl} (MPa)	F_{crg} (MPa)	$\frac{P_{crl}}{P_u}$
1.372-152-305	0.145	388.0	80.6	101.4	159.2	0.880
1.372-152-610	0.290	388.0	80.4	101.4	155.2	0.882
1.372-152-762	0.363	388.0	79.7	101.4	154.4	0.890
1.372-152-914	0.435	388.0	68.9	101.4	149.9	1.029
1.155-92-305	0.145	297.1	61.1	184.2	205.4	1.355
1.155-92-610	0.290	297.1	51.2	184.2	200.2	1.617
1.155-92-914	0.435	297.1	51.8	184.2	192.3	1.600
0.88-92-305	0.145	205.3	35.9	97.9	193.3	0.927
0.88-92-610	0.290	205.3	39.6	97.9	188.2	0.842
0.88-92-914	0.435	205.3	38.9	97.9	181.3	0.858
0.841-152-305	0.145	266.5	35.5	36.2	138.9	0.426
0.841-152-610	0.290	266.5	40.4	36.2	136.2	0.374
0.841-152-914	0.435	266.5	33.7	36.2	132.1	0.449

Table A2. Analysis of back-to-back channel sections used in Zhang and Young [16], Craverio et al. [25] and Lu et al. [26] with global buckling stress (F_{crg}) computed using CoSFSM framework

Specimen	$\frac{s}{KL}$	F_y (MPa)	P_u (kN)	F_{crl} (MPa)	F_{crg} (MPa)	$\frac{P_{crl}}{P_u}$
IT1L3200	0.063	500.0	71.1	829.1	236.7	4.862
IT1.2L2600	0.077	500.0	149.6	1188.0	358.8	3.983
IT1.2L3200	0.063	500.0	105.3	1188.0	239.3	5.659
I-PP	0.246	280.0	75.6	306.9	85.1	5.193
I-FF	0.492	280.0	187.0	306.9	286.4	2.101
LC3-90-A	0.100	322.0	41.2	203.7	107.9	2.432
LC3-140-A	0.100	305.0	48.8	143.9	84.3	2.249
IT1L3200	0.063	500.0	71.1	829.1	236.7	4.862

Table A3. Analysis of back-to-back channel sections used in Roy et al. [23] with global buckling stress (F_{crg}) computed using CoSFSM framework

Specimen	$\frac{s}{KL}$	F_y (MPa)	P_u (kN)	F_{crl} (MPa)	F_{crg} (MPa)	$\frac{P_{crl}}{P_u}$
BU75_S225_L1000	0.199	560.0	46.7	272.7	150.6	1.894
BU75_S450_L1000	0.397	560.0	45.7	270.1	139.4	1.914
BU75_S900_L1000	0.794	560.0	35.0	268.3	98.0	2.482
BU75_S475_L2000	0.217	560.0	10.9	270.1	39.0	8.066
BU75_S950_L2000	0.435	560.0	8.7	268.3	38.6	9.993
BU75_S1900_L2000	0.870	560.0	7.6	268.3	26.7	11.513
BU75_S225_L1133_t0.75	0.199	560.0	23.4	110.6	131.8	0.986
BU75_S225_L1133_t0.8	0.199	560.0	25.4	133.6	138.5	1.170
BU75_S225_L1133_t0.85	0.199	560.0	27.4	148.2	138.7	1.278
BU75_S225_L1133_t0.9	0.199	560.0	29.4	168.4	145.8	1.433
BU75_S225_L1133_t0.95	0.199	560.0	31.3	185.0	147.1	1.561
BU75_S225_L1133_t1	0.199	560.0	33.1	187.4	148.0	1.529
BU75_S225_L1133_t1.05	0.199	560.0	34.9	211.7	148.7	1.719
BU75_S225_L1133_t1.1	0.199	560.0	36.7	232.1	149.5	1.879
BU75_S225_L1133_t1.15	0.199	560.0	38.4	253.5	149.9	2.050
BU75_S225_L1133_t1.2	0.199	560.0	40.3	272.7	150.5	2.192
BU75_S225_L1133_t1.25	0.199	560.0	42.1	299.1	151.1	2.398
BU75_S225_L1133_t1.3	0.199	560.0	43.8	323.2	151.5	2.590
BU75_S225_L1133_t1.35	0.199	560.0	45.6	348.2	152.0	2.783
BU75_S225_L1133_t1.4	0.199	560.0	47.4	373.9	152.3	2.982
BU75_S225_L1133_t1.45	0.199	560.0	49.2	400.5	152.9	3.187
BU75_S225_L1133_t1.5	0.199	560.0	51.0	427.6	153.2	3.396
BU75_S225_L1133_t1.55	0.199	560.0	52.7	460.2	153.5	3.654
BU75_S225_L1133_t1.6	0.199	560.0	54.5	490.0	154.1	3.884
BU75_S225_L1133_t1.65	0.199	560.0	56.3	520.7	154.6	4.120
BU75_S225_L1133_t1.7	0.199	560.0	58.1	552.3	155.0	4.363
BU75_S225_L1133_t1.75	0.199	560.0	59.9	584.5	155.3	4.611
BU75_S225_L1133_t1.8	0.199	560.0	61.6	617.5	155.9	4.872
BU75_S225_L1133_t1.85	0.199	560.0	63.4	651.2	156.2	5.131
BU75_S225_L1133_t1.9	0.199	560.0	65.2	685.9	156.4	5.397
BU75_S225_L1133_t1.95	0.199	560.0	67.0	721.5	157.1	5.670
BU75_S225_L1133_t2	0.199	560.0	68.7	757.9	157.4	5.957
BU75_S225_L1133_t2.05	0.199	560.0	70.5	795.1	158.0	6.243
BU75_S225_L1133_t2.1	0.199	560.0	72.3	833.1	158.3	6.534
BU75_S225_L1133_t2.15	0.199	560.0	74.1	871.6	158.8	6.828
BU75_S225_L1133_t2.2	0.199	560.0	75.8	908.8	158.9	7.122
BU75_S225_L1133_t2.25	0.199	560.0	77.6	941.2	159.4	7.368
BU75_S225_L1133_t2.3	0.199	560.0	79.4	968.1	159.9	7.572
BU75_S225_L1133_t2.35	0.199	560.0	81.2	989.5	160.2	7.732
BU75_S225_L1133_t2.4	0.199	560.0	83.0	1006.1	160.6	7.855
BU75_S225_L1133_t2.45	0.199	560.0	84.8	1019.1	161.0	7.950
BU75_S225_L1133_t2.5	0.199	560.0	86.6	1029.5	161.4	8.025
BU75_S474.5_L2184_t0.75	0.217	560.0	7.6	110.6	39.6	2.947

Table A3. Continued

Specimen	$\frac{s}{KL}$	F_y (MPa)	P_u (kN)	F_{crl} (MPa)	F_{crg} (MPa)	$\frac{P_{crl}}{P_u}$
BU75_S474.5_L2184_t0.8	0.217	560.0	8.2	133.6	39.9	3.519
BU75_S474.5_L2184_t0.85	0.217	560.0	8.8	148.2	39.8	3.865
BU75_S474.5_L2184_t0.9	0.217	560.0	9.5	168.4	39.9	4.307
BU75_S474.5_L2184_t0.95	0.217	560.0	10.1	185.0	40.1	4.698
BU75_S474.5_L2184_t1	0.217	560.0	10.7	204.9	40.3	5.169
BU75_S474.5_L2184_t1.05	0.217	560.0	11.3	229.0	40.3	5.745
BU75_S474.5_L2184_t1.1	0.217	560.0	11.8	247.6	40.5	6.232
BU75_S474.5_L2184_t1.15	0.217	560.0	12.4	270.5	40.5	6.773
BU75_S474.5_L2184_t1.2	0.217	560.0	12.9	294.4	40.7	7.394
BU75_S474.5_L2184_t1.25	0.217	560.0	13.6	319.3	40.9	7.923
BU75_S474.5_L2184_t1.3	0.217	560.0	14.1	345.1	40.9	8.591
BU75_S474.5_L2184_t1.35	0.217	560.0	14.7	372.0	41.0	9.224
BU75_S474.5_L2184_t1.4	0.217	560.0	15.3	399.8	41.1	9.878
BU75_S474.5_L2184_t1.45	0.217	560.0	15.9	428.6	41.3	10.554
BU75_S474.5_L2184_t1.5	0.217	560.0	16.4	458.4	41.3	11.321
BU75_S474.5_L2184_t1.55	0.217	560.0	17.0	489.2	41.3	12.043
BU75_S474.5_L2184_t1.6	0.217	560.0	17.6	520.9	41.5	12.787
BU75_S474.5_L2184_t1.65	0.217	560.0	18.2	553.7	41.5	13.552
BU75_S474.5_L2184_t1.7	0.217	560.0	18.7	578.1	41.7	14.189
BU75_S474.5_L2184_t1.75	0.217	560.0	19.3	610.5	41.7	14.947
BU75_S474.5_L2184_t1.8	0.217	560.0	19.9	645.5	41.9	15.764
BU75_S474.5_L2184_t1.85	0.217	560.0	20.5	681.4	41.9	16.602
BU75_S474.5_L2184_t1.9	0.217	560.0	21.0	718.2	42.1	17.544
BU75_S474.5_L2184_t1.95	0.217	560.0	21.6	755.9	42.1	18.425
BU75_S474.5_L2184_t2	0.217	560.0	22.2	794.6	42.3	19.327
BU75_S474.5_L2184_t2.05	0.217	560.0	22.8	834.1	42.4	20.249
BU75_S474.5_L2184_t2.1	0.217	560.0	23.3	874.6	42.5	21.283
BU75_S474.5_L2184_t2.15	0.217	560.0	23.9	915.9	42.6	22.247
BU75_S474.5_L2184_t2.2	0.217	560.0	24.5	958.2	42.7	23.232
BU75_S474.5_L2184_t2.25	0.217	560.0	25.0	1001.3	42.8	24.333
BU75_S474.5_L2184_t2.3	0.217	560.0	25.6	1045.4	43.0	25.358
BU75_S474.5_L2184_t2.35	0.217	560.0	26.2	1090.1	43.0	26.401
BU75_S474.5_L2184_t2.4	0.217	560.0	26.8	1134.3	43.2	27.427
BU75_S474.5_L2184_t2.45	0.217	560.0	27.4	1180.9	43.2	28.508
BU75_S474.5_L2184_t2.5	0.217	560.0	27.9	1209.1	43.3	29.252

Table A4. Analysis of back-to-back channel sections used in Zhou et al. [20] with global buckling stress (F_{crg}) computed using CoSFSM framework

Specimen	$\frac{s}{KL}$	F_y (MPa)	P_u (kN)	F_{crl} (MPa)	F_{crg} (MPa)	$\frac{P_{crl}}{P_u}$
B80-40-1	0.500	321.5	15.6	204.6	46.7	4.722
B80-40-2	0.333	321.5	16.3	204.6	51.0	4.519
B80-40-3	0.250	321.5	16.5	204.6	52.1	4.464
B80-40-4	0.200	321.5	16.6	204.6	52.6	4.437
B80-40-5	0.167	321.5	16.6	204.6	52.9	4.437
B80-40-6	0.100	321.5	16.7	204.6	53.2	4.411
B80-40-7	0.025	321.5	16.8	204.6	53.3	4.384
B80-60-8	0.500	321.5	93.0	700.9	107.3	6.632
B80-60-9	0.333	321.5	94.3	700.9	119.8	6.540
B80-60-10	0.250	321.5	95.1	700.9	123.3	6.485
B80-60-11	0.200	321.5	94.9	700.9	124.8	6.499
B80-60-12	0.167	321.5	96.6	700.9	125.7	6.385
B80-60-13	0.100	321.5	100.0	700.9	126.6	6.168
B80-60-14	0.025	321.5	101.7	700.9	127.0	6.065
B120-40-15	0.500	321.5	33.3	303.5	42.6	8.165
B120-40-16	0.333	321.5	33.6	303.5	45.9	8.093
B120-40-17	0.250	321.5	33.7	303.5	46.8	8.069
B120-40-18	0.200	321.5	34.4	303.5	47.2	7.904
B120-40-19	0.167	321.5	34.8	303.5	47.4	7.813
B120-40-20	0.100	321.5	35.5	303.5	47.7	7.659
B120-40-21	0.025	321.5	35.6	303.5	47.8	7.638
B120-60-22	0.500	321.5	130.4	451.7	104.9	4.676
B120-60-23	0.333	321.5	133.3	451.7	115.3	4.574
B120-60-24	0.250	321.5	136.2	451.7	118.2	4.477
B120-60-25	0.200	321.5	137.2	451.7	119.5	4.444
B120-60-26	0.167	321.5	138.0	451.7	120.3	4.418
B120-60-27	0.100	321.5	141.9	451.7	121.1	4.297
B120-60-28	0.025	321.5	142.8	451.7	121.5	4.270
B160-40-29	0.500	321.5	40.7	274.4	40.5	9.101
B160-40-30	0.333	321.5	41.7	274.4	43.3	8.883
B160-40-31	0.250	321.5	41.8	274.4	44.1	8.862
B160-40-32	0.200	321.5	42.7	274.4	44.5	8.675
B160-40-33	0.167	321.5	43.2	274.4	44.7	8.575
B160-40-34	0.100	321.5	44.1	274.4	44.9	8.400
B160-40-35	0.025	321.5	44.1	274.4	45.0	8.400
B160-60-36	0.500	321.5	140.0	380.3	93.9	5.052
B160-60-37	0.333	321.5	153.2	380.3	101.8	4.617
B160-60-38	0.250	321.5	155.1	380.3	104.1	4.560
B160-60-39	0.200	321.5	155.3	380.3	105.3	4.555
B160-60-40	0.167	321.5	154.2	380.3	105.8	4.587
B160-60-41	0.100	321.5	155.0	380.3	106.5	4.563
B160-60-42	0.025	321.5	155.2	380.3	106.9	4.557

Table A5. Analysis of back-to-back channel sections used in Zhang and Young [24] with global buckling stress (F_{crg}) computed using CoSFSM framework

Specimen	$\frac{s}{KL}$	F_y (MPa)	P_u (kN)	F_{crl} (MPa)	F_{crg} (MPa)	$\frac{P_{crl}}{P_u}$
I-E16A60T1.0L2200	0.091	604.0	215.0	525.8	446.6	1.404
I-E16A60T1.0L2800	0.071	604.0	175.6	525.8	447.5	1.719
I-E16A60T1.0L3400	0.059	604.0	137.9	525.8	308.7	2.188
I-E16A60T1.0L4000	0.050	604.0	104.7	525.8	225.6	2.882
I-E16A60T1.5L2200	0.091	604.0	353.6	1179.4	724.9	2.872
I-E16A60T1.5L2800	0.071	604.0	285.1	1179.4	460.1	3.562
I-E16A60T1.5L3400	0.059	604.0	216.5	1179.4	316.3	4.690
I-E16A60T1.5L4000	0.050	604.0	160.8	1179.4	230.0	6.315
I-E16A60T2.0L2200	0.091	604.0	608.8	2991.0	738.4	5.640
I-E16A60T2.0L2800	0.071	604.0	479.6	2991.0	468.9	7.159
I-E16A60T2.0L3400	0.059	604.0	354.0	2991.0	322.4	9.699
I-E16A60T2.0L4000	0.050	604.0	264.6	2991.0	234.2	12.976
I-E08A60T1.0L2200	0.091	604.0	193.9	542.8	617.1	1.517
I-E08A60T1.0L2800	0.071	604.0	158.6	542.8	407.5	1.855
I-E08A60T1.0L3400	0.059	604.0	118.0	542.8	278.9	2.493
I-E08A60T1.0L4000	0.050	604.0	89.1	542.8	203.2	3.302
I-E08A60T1.5L2200	0.091	604.0	326.0	1214.7	653.0	3.029
I-E08A60T1.5L2800	0.071	604.0	249.4	1214.7	416.4	3.960
I-E08A60T1.5L3400	0.059	604.0	186.1	1214.7	284.8	5.306
I-E08A60T1.5L4000	0.050	604.0	139.3	1214.7	206.8	7.089
I-E08A60T2.0L2200	0.091	604.0	542.8	3032.0	666.1	6.055
I-E08A60T2.0L2800	0.071	604.0	422.4	3032.0	423.3	7.781
I-E08A60T2.0L3400	0.059	604.0	311.1	3032.0	290.2	10.565
I-E08A60T2.0L4000	0.050	604.0	230.5	3032.0	210.5	14.259
I-E24A60T1.0L2200	0.091	604.0	201.0	293.3	455.3	0.884
I-E24A60T1.0L2800	0.071	604.0	167.1	293.3	469.6	1.064
I-E24A60T1.0L3400	0.059	604.0	138.1	293.3	330.5	1.287
I-E24A60T1.0L4000	0.050	604.0	111.7	293.3	243.7	1.591
I-E24A60T1.5L2200	0.091	604.0	382.4	657.7	743.1	1.563
I-E24A60T1.5L2800	0.071	604.0	312.0	657.7	492.0	1.916
I-E24A60T1.5L3400	0.059	604.0	239.9	657.7	341.6	2.491
I-E24A60T1.5L4000	0.050	604.0	184.6	657.7	249.6	3.238
I-E24A60T2.0L2200	0.091	604.0	636.6	1667.0	799.9	3.174
I-E24A60T2.0L2800	0.071	604.0	512.9	1667.0	504.8	3.939
I-E24A60T2.0L3400	0.059	604.0	399.0	1667.0	349.3	5.064
I-E24A60T2.0L4000	0.050	604.0	307.4	1667.0	254.5	6.573
I-E16A45T1.0L2200	0.091	604.0	188.2	538.9	466.6	1.529
I-E16A45T1.0L2800	0.071	604.0	137.7	538.9	333.1	2.090
I-E16A45T1.0L3400	0.059	604.0	103.7	538.9	223.3	2.775
I-E16A45T1.0L4000	0.050	604.0	72.8	538.9	164.2	3.953
I-E16A45T1.5L2200	0.091	604.0	290.2	1205.3	534.5	3.327
I-E16A45T1.5L2800	0.071	604.0	215.2	1205.3	340.8	4.486
I-E16A45T1.5L3400	0.059	604.0	152.5	1205.3	233.5	6.331

Table A5. Continued

Specimen	$\frac{s}{KL}$	F_y (MPa)	P_u (kN)	F_{crl} (MPa)	F_{crg} (MPa)	$\frac{P_{crl}}{P_u}$
I-E16A45T1.5L4000	0.050	604.0	112.8	1205.3	169.5	8.559
I-E16A45T2.0L2200	0.091	604.0	486.2	3027.3	546.6	6.650
I-E16A45T2.0L2800	0.071	604.0	358.8	3027.3	347.4	9.011
I-E16A45T2.0L3400	0.059	604.0	256.5	3027.3	238.1	12.605
I-E16A45T2.0L4000	0.050	604.0	188.4	3027.3	172.8	17.161
I-E16A30T1.0L2200	0.091	604.0	157.3	538.9	457.4	1.761
I-E16A30T1.0L2800	0.071	604.0	120.7	538.9	294.1	2.295
I-E16A30T1.0L3400	0.059	604.0	85.7	538.9	201.9	3.232
I-E16A30T1.0L4000	0.050	604.0	64.0	538.9	147.0	4.328
I-E16A30T1.5L2200	0.091	604.0	271.2	1197.3	472.6	3.404
I-E16A30T1.5L2800	0.071	604.0	199.7	1197.3	301.7	4.623
I-E16A30T1.5L3400	0.059	604.0	135.8	1197.3	206.8	6.798
I-E16A30T1.5L4000	0.050	604.0	99.4	1197.3	150.2	9.287
I-E16A30T2.0L2200	0.091	604.0	455.8	3153.0	484.2	7.111
I-E16A30T2.0L2800	0.071	604.0	320.2	3153.0	307.7	10.123
I-E16A30T2.0L3400	0.059	604.0	230.6	3153.0	210.9	14.056
I-E16A30T2.0L4000	0.050	604.0	164.8	3153.0	153.2	19.668
I-E16A00T1.0L2200	0.091	604.0	111.0	47.7	336.0	0.216
I-E16A00T1.0L2800	0.071	604.0	96.5	47.7	245.4	0.249
I-E16A00T1.0L3400	0.059	604.0	74.7	47.7	181.4	0.322
I-E16A00T1.0L4000	0.050	604.0	56.7	47.7	135.2	0.424
I-E16A00T1.5L2200	0.091	604.0	196.2	106.5	378.1	0.410
I-E16A00T1.5L2800	0.071	604.0	161.9	106.5	270.6	0.497
I-E16A00T1.5L3400	0.059	604.0	120.4	106.5	190.0	0.669
I-E16A00T1.5L4000	0.050	604.0	88.1	106.5	139.3	0.914
I-E16A00T2.0L2200	0.091	604.0	344.3	267.4	412.5	0.783
I-E16A00T2.0L2800	0.071	604.0	275.8	267.4	278.5	0.977
I-E16A00T2.0L3400	0.059	604.0	190.5	267.4	195.2	1.415
I-E16A00T2.0L4000	0.050	604.0	146.9	267.4	142.4	1.835

Table A6. Analysis of back-to-back channel sections used in Fratamico et al. [11] with global buckling stress (F_{crg}) computed using CoSFSM framework

Specimen	$\frac{s}{KL}$	F_y (MPa)	P_u (kN)	F_{crl} (MPa)	F_{crg} (MPa)	$\frac{P_{crl}}{P_u}$
A1-250S137-33	0.500	320.0	46.1	176.3	608.4	0.951
A1-250S1374	0.500	333.0	66.7	296.5	640.9	1.435
A1-250S134	0.500	395.0	113.4	467.5	629.6	1.673
A1-250S137-68	0.500	353.0	119.0	824.0	608.7	3.548
B1-362S137-33	0.500	320.0	44.3	86.8	581.4	0.596
B1-362S137-43	0.500	333.0	70.6	146.1	611.5	0.816
B1-362S137-54	0.500	395.0	102.9	230.5	647.5	1.111
B1-362S137-68	0.500	353.0	115.8	364.4	668.9	1.971
C1-600S137-33	0.500	320.0	50.2	32.6	451.4	0.263
C1-600S137-43	0.500	333.0	78.6	55.1	459.3	0.368
C1-600S137-54	0.500	395.0	103.0	86.3	442.7	0.553
C1-600S137-68	0.500	353.0	151.0	134.8	446.7	0.745
D1-600S162-33	0.500	320.0	49.2	33.8	681.0	0.300
D1-600S162-43	0.500	333.0	71.9	59.9	684.9	0.471
D1-600S162-54	0.500	395.0	137.6	89.4	696.8	0.462
D1-600S162-68	0.500	353.0	174.4	141.7	688.1	0.729

Acknowledgements

The authors wish to thank Queensland University of Technology (Australia), Indian Institute of Technology Madras (India) and Australian Research Council (Grant Number LP170100951) for providing financial support and research facilities and support.

References

[1] AISI S100, 2016. North American Specification for the design of cold-formed steel structural members. American Iron and Steel Institute (AISI), Washington, DC.

[2] AS/NZS 4600, 2018. Cold-formed steel structures. Standards Australia/Standards New Zealand, Sydney, NSW, Australia.

[3] Schafer, B. W., 2002. Local, distortional, and Euler buckling of thin-walled columns. *Journal of structural engineering*, 128(3), 289-299. https://doi.org/10.1061/(ASCE)0733-9445(2002)128:3(289)

[4] Young, B., Silvestre, N., and Camotim, D., 2013. Cold-formed steel lipped channel columns influenced by local-distortional interaction: strength and DSM design. *Journal of Structural Engineering*, 139(6), 1059-1074. https://doi.org/10.1061/(ASCE)ST.1943-541X.0000694

[5] Landesmann, A., Camotim, D., and Garcia, R., 2016. On the strength and DSM design of cold-formed steel web/flange-stiffened lipped channel columns buckling and failing in distortional modes. *Thin-Walled Structures*, 105, 248-265. https://doi.org/10.1016/j.tws.2016.03.023

[6] Peköz, Teoman., 1986. Development of a Unified Approach to the Design of Cold-formed Steel Members (Draft). *AISI Specifications for the Design of Cold-Formed Steel Structural Members. 40*. http://scholarsmine.mst.edu/ccfss-aisi-spec/40

[7] Gunalan, S., and Mahendran, M., 2013. Improved design rules for fixed ended cold-formed steel columns subject to flexural–torsional buckling. *Thin-Walled Structures*, 73, 1-17. https://doi.org/10.1016/j.tws.2013.06.013

[8] Dinis, P. B., Camotim, D., Landesmann, A., and Martins, A. D., 2019. On the direct strength method design of columns against global failures. *Thin-Walled Structures*, 139, 242-270. https://doi.org/10.1016/j.tws.2019.02.027

[9] Rajkannu, J. S., and Jayachandran, S. A., 2020. Flexural-torsional buckling strength of thin-walled channel sections with warping restraint. *Journal of Constructional Steel Research*, 169, 106041. https://doi.org/10.1016/j.jcsr.2020.106041

[10] AISC 360, 2016. Specification for Structural Steel Buildings. American Institute of Steel Construction (AISC).

[11] Fratamico, D. C., Torabian, S., Zhao, X., Rasmussen, K. J., and Schafer, B. W., 2018. Experiments on the global buckling and collapse of built-up cold-formed steel columns. *Journal of Constructional Steel Research*, *144*, 65-80. https://doi.org/10.1016/j.jcsr.2018.01.007

[12] Li, Y., Li, Y., Wang, S. and Shen, Z., 2014. Ultimate load-carrying capacity of cold-formed thin-walled columns with built-up box and I section under axial compression. *Thin-Walled Structures*, 79, pp.202-217. https://doi.org/10.1016/j.tws.2014.02.003

[13] Stone, T. A., and LaBoube, R. A., 2005. Behaviour of cold-formed steel built-up I-sections. *Thin-Walled Structures*, 43(12), 1805–1817. https://doi.org/10.1016/j.tws.2005.09.001

[14] Schafer, B. W., and Ádány, S., 2006. Buckling analysis of cold-formed steel members using CUFSM: Conventional and constrained finite strip methods. In: *18th International Specialty Conference on Cold-Formed Steel Structures: Recent Research and Developments in Cold-Formed Steel Design and Construction*, Johns Hopkins University, United States, 39–54.

[15] Young, B., and Chen, J., 2008. Design of Cold-Formed Steel Built-Up Closed Sections with Intermediate Stiffeners. *Journal of Structural Engineering*, 134(May), 727–737. https://doi.org/10.1061/(ASCE)0733-9445(2008)134:5(727)

[16] Zhang, J. H. and Young, B., 2012. Compression tests of cold-formed steel I-shaped open sections with edge and web stiffeners, *Thin-Walled Structures*, 52,1-11. https://doi.org/10.1016/j.tws.2011.11.006

[17] Fratamico, D. C., Torabian, S., and Schafer, B. W., 2015. Composite Action in Global Buckling of Built-Up Columns Using Semi-Analytical Fastener Elements. In *Proc. of the Annual Stability Conf., Structural Stability Res. Co., Nashville, TN*.

[18] Abbasi, M., Khezri, M., Rasmussen, K.J.R. and Schafer, B.W., 2018. Elastic buckling analysis of cold-formed steel built-up sections with discrete fasteners using the compound strip method. *Thin-Walled Structures*, 124, pp.58-71. https://doi.org/10.1016/j.tws.2017.11.046

[19] Puckett, J. A. and Wiseman D. L., 1991. Compound strip method for folded plates with connecting elements, *Journal of Structural Engineering*, 117 (1), 255–267. https://doi.org/10.1061/(ASCE)0733-9445(1991)117:1(255)

[20] Zhou, T., Li, Y., Wu, H., Lu, Y., and Ren, L., 2020. Analysis to determine flexural buckling of cold-formed steel built-up back-to-back section columns. *Journal of Constructional Steel Research*, *166*, 105898. https://doi.org/10.1016/j.jcsr.2019.105898

[21] Rasmussen, K.J., Khezri, M., Schafer, B.W. and Zhang, H., 2020. The mechanics of built-up cold-formed steel members. *Thin-Walled Structures*, 154, p.106756. https://doi.org/10.1016/j.tws.2020.106756

[22] Mahar, A.M. and Jayachandran, S. A., 2021. A Computational Study on Buckling Behavior of Cold-Formed Steel Built-Up Columns Using Compound Spline Finite Strip Method. *International Journal of Structural Stability and Dynamics*, p.2150064. https://doi.org/10.1142/S0219455421500644

[23] Roy, K., Ting, T. C. H., Lau, H. H., and Lim, J. B., 2018. Effect of thickness on the behaviour of axially loaded back-to-back cold-formed steel built-up channel sections-Experimental and numerical investigation. *Structures* Vol. 16, pp. 327-346. https://doi.org/10.1016/j.istruc.2018.09.009

[24] Zhang, J.H. and Young, B., 2015. Numerical investigation and design of cold-formed steel built-up open section columns with longitudinal stiffeners. *Thin-Walled Structures*, 89, pp.178-191.

[25] Craveiro, H. D., Rodrigues, J. P. C., and Laím, L., 2016. Buckling resistance of axially loaded cold-formed steel columns. *Thin-Walled Structures*, *106*, 358-375. https://doi.org/10.1016/j.tws.2016.05.010

[26] Lu, Y., Zhou, T., Li, W., and Wu, H., 2017. Experimental investigation and a novel direct strength method for cold-formed built-up I-section columns. *Thin-Walled Structures*, *112*, 125-139. https://doi.org/10.1016/j.tws.2016.12.011

[27] AISC-LRFD, 1986. Manual of Steel Construction: Load and Resistance Factor Design Manual of Steel Construction. American Institute of Steel Construction.

[28] Zandonini, R., 1985. Stability of compact built-up struts: experimental investigation and numerical simulation. *Construzioni metalliche*, (4), 288.

[29] Astaneh-Asl, A., Goel, S.C. and Hanson, R.D., 1985. Cyclic out-of-plane buckling of double-angle bracing. *Journal of Structural Engineering*, 111(5), pp.1135-1153. https://doi.org/10.1061/(ASCE)0733-9445(1985)111:5(1135)

[30] Duan, L., and Chen, W. F., 1988. Design rules of built-up members in load and resistance factor design. *Journal of Structural Engineering*, 114(11), 2544-2554. https://doi.org/10.1061/(ASCE)0733-9445(1988)114:11(2544)

[31] Lau, S. C. W., and Hancock, G. J., 1986. Buckling of thin flat-walled structures by a spline finite strip method. *Thin-walled structures*, *4*(4), 269-294. https://doi.org/10.1016/0263-8231(86)90034-0

[32] Eccher, G., Rasmussen, K. J. R., and Zandonini, R., 2008. Elastic buckling analysis of perforated thin-walled structures by the isoparametric spline finite strip method. *Thin-Walled Structures*, 46(2), 165-191. https://doi.org/10.1016/j.tws.2007.08.030

[33] Ajeesh, S.S. and Jayachandran, S. A., 2017. Identification of buckling modes in generalised spline finite strip analysis of cold-formed steel members. *Thin-Walled Structures*, 119, pp.593-602. https://doi.org/10.1016/j.tws.2017.07.005

[34] Chen, C. J., Gutkowski, R. M., and Puckett, J. A., 1991. B-spline compound strip formulation for braced thin-walled structures. *Journal of Structural Engineering*, 117(5), 1303-1316. https://doi.org/10.1061/(ASCE)0733-9445(1991)117:5(1303)

[35] Ajeesh, S.S. and Jayachandran, S. A., 2017. Amendment schemes for cubic end splines used in structural analysis. *Journal of Structural Engineering (India)*, 43(6), pp. 539-546

[36] Kumar, M. V. A. 2012. Interaction of local, distortional and overall buckling in cold-formed steel lipped channel compression members. Ph.D. thesis, Indian Institute of Technology Madras, Chennai, India.

[37] ABAQUS 2014. *ABAQUS Analysis user's manual*, *Version 6.14*. Dassault Systèmes Simulia Corp, Providence, RI, USA.

[38] EN 1993-1-3, 2006. Eurocode 3- Design of Steel Structures- Part 1- 3: General rules-Supplementary rules for cold-formed members and sheeting.